AD-A267 476

REPOR

Form Approved
OMB No. 0704-0188

Public reporting burden for this collec gathering and maintaining the data n collection of information, including si Davis Highway, Suite 1204, Arlington, ... --

ing the time for reviewing instructions, searching existing data sources, nd comments regarding this burden estimate or any other aspect of this ces, Directorate for Information Operations and Reports, 1215 Jefferson ork Reduction Project (0704-0188), Washington, DC 20503.

1. AGENCY USE ONLY (Leave blank)	2. REPORT DATE	3. REPORT TYPE AND DATES COVERED
	June 6, 1993	Final Technical Rept. 01/01/90-12/31/92

4. TITLE AND SUBTITLE

Structure of high Reynolds number turbulent boundary layer

5. FUNDING NUMBERS

G-X

AFOSR-90-0120

6. AUTHOR(S)

K.R. Sreenivasan

7. PERFORMING ORGANIZATION NAME(S) AND ADDRESS(ES)

Yale University
9 Hillhouse Ave.
New Haven, CT 06520-2159

8. PERFORMING ORGANIZATION REPORT NUMBER

AFOSR-TR- 93 0471

9. SPONSORING/MONITORING AGENCY NAME(S) AND ADDRESS(ES)

NA

AFOSR/NA
Building 410
Bolling Air Force Base, D.C. 20332-6448

10. SPONSORING/MONITORING AGENCY REPORT NUMBER

AFOSR-90-0120

11. SUPPLEMENTARY NOTES

--

12a. DISTRIBUTION/AVAILABILITY STATEMENT

Approved for public release; distribution is unlimited

12b. DISTRIBUTION CODE

UL

13. ABSTRACT *(Maximum 200 words)*

A brief summary of the work done at Yale in the collaborative research program between Yale, Princeton and Penn State is given. One of the findings of the work is that there is a second-order "transition" between the low-Reynolds-number boundary layer and the high-Reynolds-number boundary layer. The nature of this transition and the elucidation of this mechanism is one of the topics of this research. Other aspects concern the self-similar scaling aspects of the Reynolds shear stress, scaling of the probability density of velocity increments and the scaling of the multiplier distributions for the energy dissipation.

93-17692

DTIC
AUG 05 1993

14. SUBJECT TERMS	15. NUMBER OF PAGES
High-Reynolds-number turbulent boundary layer, velocity increments, multiplier distributions	7 + two reprints
	16. PRICE CODE: --

17. SECURITY CLASSIFICATION OF REPORT	18. SECURITY CLASSIFICATION OF THIS PAGE	19. SECURITY CLASSIFICATION OF ABSTRACT	20. LIMITATION OF ABSTRACT
unclassified	unclassified	unclassified	UL

NSN 7540-01-280-5500

Standard Form 298 (Rev. 2-89)
Prescribed by ANSI Std. Z39-18

93 8 3 288

FINAL TECHNICAL REPORT

submitted to

Air Force Office of Scientific Research

for the grant AFOSR-90-0120

High Reynolds number turbulent boundary layer

by

K.R. Sreenivasan

Department of Mechanical Engineering

Mason Laboratory, Yale University

New Haven, CT 06520

June 6, 1993

1. Introduction

This project entitled: 'The structure of high-Reynolds-number turbulent boundary layer' was a collaborative effort between Yale (PI: K.R. Sreenivasan), Princeton (PI: A.J. Smits) and Penn. State (PI: J. Brasseur). The main point of the proposal was that the structure of the high-Reynolds-number turbulent boundary layer may differ substantially from that at moderate Reynolds numbers, and is therefore worth a special look.

The emphasis in this project - which involved experiment, simulations and data analysis - was to be on aspects such as: (a) in what respects does the boundary layer at high Reynolds numbers differ from that at low Reynolds numbers? (b) What mechanisms in particular contribute to turbulent transport of heat, mass and momentum in the logarithmic region? (c) What sets the scales for transport in the boundary layer? (d) Is the transport primarily in the form of some small number of very active events occupying small amounts of time (and space), or does it occur over most of the time (and occupy most of the space) in a fashion that is not spectacular? (e) How can the transport phenomenon be modelled for use in sub-grid scale models? (f) What analogies from other branches of physical sciences can be brought to bear on the transport issue? Although questions concerning energy dissipation, velocity increments, zero-crossings, fractal dimensions, were to be addressed, the central part of the work was to be on turbulent transport. Progress made at Yale on these and related questions will be described here briefly.

2. Notes on the Yale work

(a) Data were acquired in the laboratory as well as atmospheric boundary layer. Atmospheric data were obtained at a few selected heights above a wheat-field canopy. They were primarily in the form of 'single point' measurements. The quantities measured were velocity components (two), the Reynolds shear stress, vorticity (streamwise component) and temperature. 'Flow visualization' was done by using smoke bombs (generally lasting for about three minutes) at several heights. Laboratory data were comparable.

(b) The multiplier method was develeoped for displaying scale-similarity in the momentum transport process at high Reynolds numbers; new schemes for the fractal analysis of turbulent velocity and temperature data in the atmospheric surface layer were also developed and used.

(c) The issue of incomplete similarity (Barenblatt, J. Fluid Mech. 248, 513, 1993) was examined in so far it bears on the mean velocity distribution in high-Reynolds-number pipe flows and boundary layers.

(d) The Reynolds number effects on the inner-outer interactions were investigated, especially on the Reynolds shear stress.

(e) Several statistical properties were examined over a wide range of Reynolds numbers; these included the probability density function (pdf) of the zero-crossing intervals in turbulent signals, and the pdf of velocity increments.

(f) The scalar field as well as velocity data were mapped out in two-dimensional planes (the latter using PIV techniques) in a moderate-Reynolds-number boundary layer. The reason for the moderate-Reynolds-number measurements is that it can be probed in much greater detail than is possible (for technical reasons) at high Reynolds numbers, and that the data so obtained may serve as a basis for comparison with the high-Reynolds-number data. It would similarly serve well for the examination of the Reynolds number effects.

3. Some further details

(a) Investigation of the skin friction data in pipes and boundary layers indicated that there might be a reasonably well-defined 'transition' between the low Reynolds number behavior and the high Reynolds number behavior. Velocity profiles as well as pressure fluctuations seemed to support the notion that a weak, or second-order, transition may indeed occur at a fairly high Reynolds number. This Reynolds number for the boundary layer is of the order of 6000 in terms of the momentum thickness, or for the pipe of the order of about 10^5 in terms of the pipe diameter. The following physical effects were considered as possible causes for this 'transition', and their relative effects were investigated.

(i) It is possible that these effects could arise because the importance of the viscous-influenced interface in the outer region could become weak beyond some Reynolds number. Fractal estimates and zero-crossing measurements precluded such a possibility.

(ii) It is possible that the localization of the energy dissipation in the outer region may be the cause. But multifractal estimates show that this is an unlikely because the localization is extremely slow in Reynolds number.

(iii) It is possible that these effects could come from the altered circumstances of the inner/outer interaction. It was first shown by an analysis of rough-pipe data that the really important parameter is not the Reynolds number but the ratio of the inner scale to the outer scale. This ratio is the same as the Reynolds number in the smooth-wall flows, but it can be prescribed independent of the Reynolds number for flows with rough walls. Thus, the so-called Reynolds number effects are really the effects of the outer/inner scale ratio. This also suggests that a study of the high-Reynolds-number dynamics is not ideally studied in the atmospheric boundary layer over rough terrain where, even though the Reynolds number is large, the effective scale ratio is not so large.

(b) It is shown that for large values of the outer/inner scale ratio, as opposed to the case of moderate values of this ratio, the velocity-conditioned Reynolds shear stress changes its character.

(c) It is shown that multiplicative representations of the Reynolds stress, in spite of some advantages of interpretation, has several problems in the logarithmic region of the boundary layer. In any case, scale-similar ranges for the multiplier distribution of the Reynolds shear stress have been identified.

(d) It is shown by investigating the instantaneous momentum fluxes that, on the average, the contributions to the Reynolds stress comes from medium amplitude velocity fluctuations of the order of 1.5 root-mean-square value. Thus very large velocity amplitudes do not contribute much to the Reynolds stress.

4. Publications

Most of this work can be found in the following references:

(a) P. Kailasnath, K.R. Sreenivasan and G. Stolovitzky, "Probability density of velocity increments in turbulent flows", Phys. Rev. Lett. 68, 2766, 1992

(b) A.B. Chhabra and K.R. Sreenivasan, "Scale-invariant multiplier distributions in turbulence", Phys. Rev. Lett. 68, 2762, 1992

(c) K.R. Sreenivasan and A. Juneja, "Fractal dimensions of time series in turbulent flows", submitted to J. Fluid Mech., 1992

(d) P. Kailasnath and K.R. Sreenivasan, "Zero-crossings of velocity fluctuations in turbulent boundary layers", submitted to Phys. Fluids A., 1992

(e) P. Kailasnath, "Studies of Reynolds number effects in turbulent boundary layers", Ph.D. thesis, Yale University, June 1993

The papers (a) and (b) are enclosed. Items (c), (d) and (e) are in the process of being published and, once published, copies will be sent to AFOSR. Most of the material central to the proposal is contained in item (e).

5. Collaboration with Princeton and Penn. State

The collaborative aspect of the work proposed between Yale, Penn. State and Princeton. This collaboration is still continuing (even though the project has formally ended), and it is expected that a few significant publications will arise from it. The collaboration has taken the form of exchange of data, mutual visits and coordination of flow conditions between simultaions and experiments. In terms of concrete results, we may cite the following aspects:

(a) Comparison of the inertial region of a high-Reynolds-number turbulent boundary layer with homogeneous shear flow;

(b) Wavelet analysis of the experimental as well as numerically generated data in boundary layers;

(c) Comparison between the simulations and experiments in moderate-Reynolds-number boundary layers.

A draft of a paper on item (a) is available, and (a) as well as (b) have been presented at APS/DFD meetings, as well as elsewhere. It will be several more months before journal publications materialize.

6. Aspects of the work that were not successful

(a) We had proposed to make measurements in high-Reynolds-number boundary layer in the new wind-tunnel facility that was to have been completed at Illinois Institute of Technology about two or three years ago. Unfortunately, this was not possible because the wind tunnel is still unfinished as of this writing. So we made progress on all other fronts available to us: acquisition and analysis of data in the high-Reynolds-number atmospheric surface layer (already mentioned), examination of the high-Reynolds-number mean velocity data acquired at APL of Penn. State, use of some relatively high-Reynolds-number data acquired at Princeton, and a study of the moderate Reynolds number data acquired by us. To supplement the analysis, we also examined all previous data obtained elsewhere, in both boundary layers and pipe flows.

(b) We had planned on obtaining the scalar and velocity fields simultaneously at moderate Reynolds numbers, but did not have the time to complete these measurements before the project came to an end, and the post-doctoral fellow working on the problem had to be terminated. Unfortunately, much time and effort was invested in this work. The consolation is that the expertise acquired will be of use in subsequent work.

7. Personnel

Besides the PI, much of the work on this project was done by a post-doctoral fellow, Dr. A.K. Suri (who made most of the scalar and PIV measurements in moderate-Reynolds-number boundary layers), and a graduate student, Mr. P. Kailasnath (who took a large share of the responsibility for single-point measurements in laboratory as well as atmospheric boundary

layers). Kailasnath has just completed his Ph.D. thesis and has taken up a position at the Yale medical School. Off and on, as demanded by circumstances, other people were employed on short-term basis. Some of the work related to the vorticity measurements in the atmospheric boundary layer are contained in the Ph.D. dissertation of Mark S. Fan. Mark's thesis was only partly supported by another grant AFOSR-87-0116. He now works for NASA.

A final note: There are several aspects of this work that are yet to be digested fully, and it is our responsible belief that more new results will appear out of this work in due course.

Scale-Invariant Multiplier Distributions in Turbulence

Ashvin B. Chhabra[1,2] and K. R. Sreenivasan[1]

[1]*Mason Laboratory, Yale University, New Haven, Connecticut 06520-2159*

[2]*Mathematical Disciplines Center and The James Franck Institute, The University of Chicago, Chicago, Illinois 60637*

(Received 4 November 1991)

A family of scale-invariant, base-dependent, multiplier distributions is measured for the turbulence dissipation field in the atmospheric surface layer. The existence of these distributions implies the existence of the more traditional multifractal scaling functions, and we compute both positive and negative parts of the $f(\alpha)$ curve. The results support the conjecture of universality in the scaling properties of small-scale turbulence. A simple cascade model based on the measured multiplier distributions is shown to possess several advantages over previously considered models.

PACS numbers: 47.25.−c, 02.50.+s, 03.40.Gc, 05.45.+b

The multifractal formalism [1–5] [e.g., the $f(\alpha)$ function] compactly describes the scaling properties of measures which arise in a variety of problems such as chaotic dynamical systems [6], diffusion-limited aggregation (DLA) [7], and dissipationlike quantities in fully developed turbulence [8]. The $f(\alpha)$ function is a macroscopic feature of such measures, and a quest for deeper understanding of the underlying physics has led to microscopic descriptions. A successful example is the Feigenbaum scaling function (FSF) [9] appropriate to the onset of chaos in the period-doubling route. Basic to the FSF are the contraction ratios (or multipliers), which describe how distances between the nearest-neighbor iterates scale with increasing levels of refinement. The FSF organizes these multipliers according to the natural time of the system described by the closest return times, and compactly describes the local scaling. The FSF description is much richer than that embodied in $f(\alpha)$, and the latter is easily computable from the former. Further, the $f(\alpha)$ description is degenerate and a variety of scaling functions lead to the same $f(\alpha)$ function [10,11].

Many multifractal measures, such as the spatial distribution of the energy dissipation rate in fully developed turbulence, or the harmonic measure of the DLA structures, display statistical properties that are different from those of deterministic systems. Two such properties are the sample-to-sample fluctuations of the $f(\alpha)$ function, and the existence of negative dimensions—both of which represent the same underlying phenomenon [12,13]. Recall that, if $P_i(\varepsilon)$ is the measure in the ith box of size ε, one can decompose the multifractal measure into interwoven sets of varying singularity strengths α (where $[P_i(\varepsilon)]^q \sim \varepsilon^{q\alpha_i}$), whose fractal dimensions $f(\alpha)$ are defined by $N(\alpha) \sim \varepsilon^{-f(\alpha)}$, $N(\alpha)$ being the number of singularities of strength α. Figure 1 shows how $f(q=2)$ and $\alpha(q=2)$, computed from the turbulence dissipation data using the direct method of Ref. [14], vary from one sample to another; each sample is approximately one macroscale in extent and produces extended and unambiguous scaling. The sample-to-sample fluctuations [15] are much larger than the least-squares errors in calculating $f(q)$ and $\alpha(q)$ from individual samples. In addition, for any given q, $f(q)$ and $\alpha(q)$ from different samples are correlated and fall along a thin band [16].

These phenomena are absent in deterministic processes, and their occurrence reflects an inherently probabilistic dynamics. For such cases, a complete specification of the scaling properties, even at the level of $f(\alpha)$, requires measuring both positive and negative parts of $f(\alpha)$ [12,13,17–20]. Negative $f(\alpha)$ for turbulent flows at moderate Reynolds numbers have already been obtained in Ref. [20] but, for atmospheric flows, their computation by conventional box-counting methods requires an enormous amount of data, involving perhaps several years of data acquisition [12,13,20]. Recently [12,13,21], a

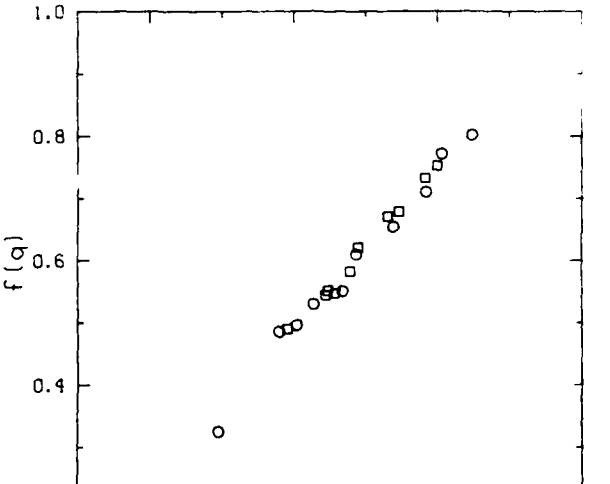

FIG. 1. Sample-to-sample fluctuations of $f(q=2)$ vs $\alpha(q=2)$ for ten samples (7200 points each, roughly equivalent to an integral scale) from an atmospheric boundary layer (squares). The circles are from a simulation of a binary cascade model with multipliers chosen randomly from a triangular distribution. This model is described later in the text (see also Fig. 2).

method based on scale-invariant multiplier distributions has been proposed as being exponentially faster and more accurate than box-counting methods. Utilizing this method, we were able to compute negative dimensions for atmospheric flows as well as a variety of model cascade processes.

This paper has several related objectives. As a continuation of the notion that scale-invariant multiplier distributions are fundamental functions, we compute them for atmospheric turbulence by assuming that the observed scaling could result from cascades of any base (binary, ternary, etc.). Using these distributions, we construct several base-independent functions such as $f(\alpha)$. We then show that the $f(\alpha)$ functions computed from different multiplier distributions agree well with each other, as well as with those computed in moderate-Reynolds-number flows by box-counting methods. Finally, we propose a relatively simple cascade model that reproduces not only the observed positive and negative parts of $f(\alpha)$ and sample-to-sample fluctuations, but also the stretched exponential tails in the probability distribution of turbulence dissipation. The superiority of the multiplier method allows us to compute $f(\alpha)$ with greater accuracy and to assess, for the first time, the universality conjecture about scaling properties in the negative-dimension range.

To compute the scale-invariant multiplier distributions one first constructs a measure which, in the present case, is the energy dissipation rate represented by the square of the derivative of a component of the velocity. The measure is then covered by boxes of uniform size. Each of these boxes is then subdivided into a number of boxes, a, and the ratios of the measures in the original box to those in the smaller sub-boxes are computed. A histogram of these ratios is then $P_a(M_a)$. Figure 2 shows $P_a(M_a)$ obtained by assuming cascades of bases $a=2$, 3, and 5. The larger symbols show an average over steps involving comparisons between boxes of size m and those of size ma, where m ranged from 50 to 1000. The shape of the distribution remains invariant for the inertial range of scales. (For the smallest scales, the distributions have a concave shape. This concavity is related to the divergence of moments [22] and will be discussed elsewhere. For very large boxes, multiplier distributions become flatter, as would be the case for random measures.)

The multiplier distributions $P_a(M_a)$ are more basic than the $f(\alpha)$ function, and were introduced in the context of turbulence by Novikov [1], and measured by Van Atta and Yeh [23]. However, their importance with regard to multifractals in turbulence has subsequently been ignored. One can compute from the multiplier distributions both the positive and negative parts of the $f(\alpha)$ function, i.e., they contain information on the asymptotic scaling properties of a measure and on fluctuations of scaling properties for samples of finite size. In addition, even in instances where high-order moments diverge [2,22], $P_a(M_a)$ remains well defined. Finally, the $f(\alpha)$

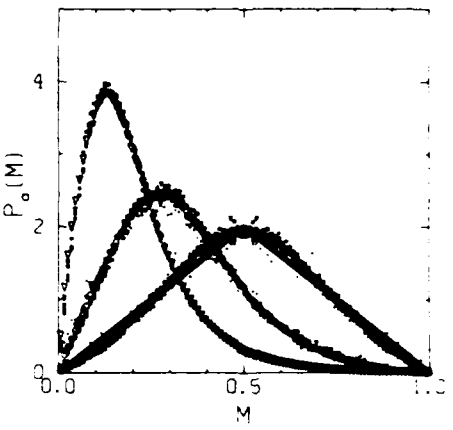

FIG. 2. Multiplier distributions $P_a(M_a)$ for bases (from right to left) $a=2$, 3, and 5. The larger symbols show averages over steps comparing measures in boxes of size m with those in size ma, $50<m<1000$ in units of the Kolmogorov scale. The smaller symbols show the distributions obtained for different values of m (50, 80, 150, 200, 400, and 1000). The solid line is a useful approximation to the $a=2$ distribution.

function may extend over $(-\infty,\infty)$ whereas $P_a(M_a)$ is a compact function defined on $M_a\in[0,1]$. The base dependency of $P_a(M_a)$ can be scaled out because the multiplier distributions corresponding to different bases are related by convolution, provided the multipliers at successive cascades are uncorrelated. With this assumption, several base-independent functions can be constructed from the multiplier distributions.

Consider as an example the Mellin transforms $\mathbf{M}$ of $P_a(M_a)$ and of its convolution $P_a^2(N)$, where N is the product of two multipliers picked according to their probabilities $P_a(M_a)$. Since the Mellin transform of a convolution is the product of the individual Mellin transforms, we have

$$\mathbf{M}\{P_{b=a}^2(M_b)\}=\mathbf{M}\{P_a(M_a)\}\cdot\mathbf{M}\{P_a(M_a)\}=[\mathbf{M}\{P_a(M_a)\}]^2. \quad (1)$$

It is clear that, in general, the exponent in the last term of Eq. (1) is simply $\log(b)/\log(a)$, the number of times the variable is being convolved. So far, for any two different bases we have

$$[\mathbf{M}\{P_a(M_a)\}]^{[1/\log(a)]}=[\mathbf{M}\{P_b(M_b)\}]^{[1/\log(b)]}. \quad (2)$$

On evaluating the Mellin transform and taking logarithms of both sides, we get [1]

$$\frac{\log\langle(M_a)^q\rangle}{\log(a)}=\frac{\log\langle(M_b)^q\rangle}{\log(b)}=-[\tau(q)+D_0]. \quad (3)$$

The other scaling functions $f(q)$, $\alpha(q)$, and D_q are simply related to $\tau(q)$, and so they too can be easily derived from the multiplier distributions. Further, one can derive equivalent scaling functions by using Laplace or Fourier transforms.

We now compute the $f(\alpha)$ function from the multiplier

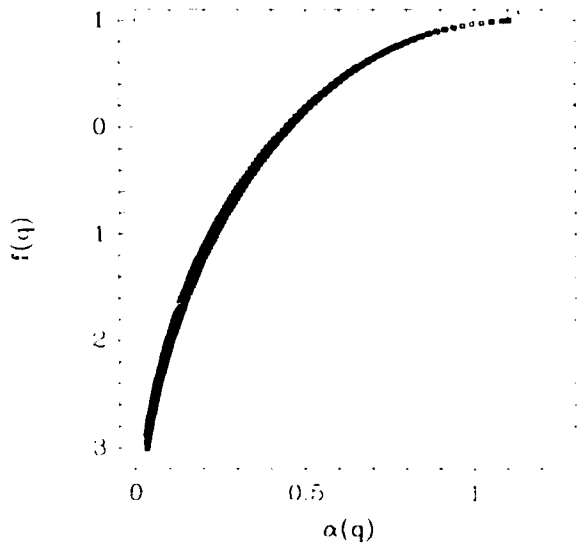

FIG. 3. The $f(\alpha)$ function from the atmospheric data for bases 2, 3, 4, 5, 6, 8, and 10, after the base-dependent prefactor has been removed. The good collapse implies that the assumption of random multiplicative processes is essentially correct, and that no single base is preferred.

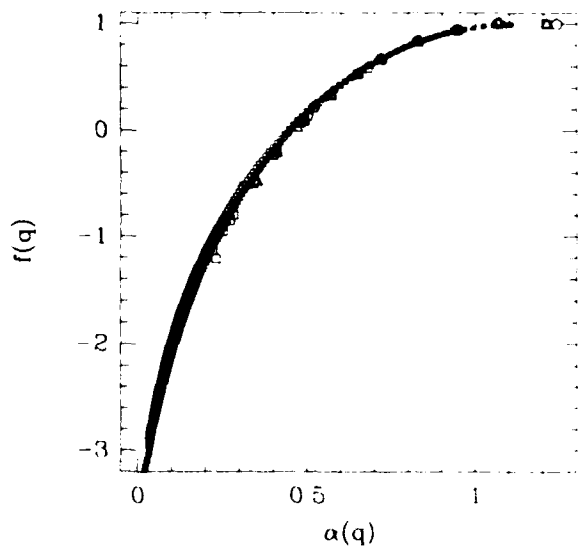

FIG. 4. The $f(\alpha)$ function for the atmospheric data for bases 2 and 10. Also reproduced (from Ref. [20]) are the data from a variety of laboratory flows (larger symbols). The small diamonds are from computations [28] using multipliers from the triangular distribution shown in Fig. 2. The agreement between $f(\alpha)$ functions for atmospheric turbulence and for laboratory flows supports the notion of universality of scaling properties at different Reynolds numbers even of the most rare events.

distributions of Fig. 2, and verify that the multifractal scaling functions derived from different-base multiplier distributions indeed collapse. While doing so, it is important to account for the existence of a prefactor in $\langle (M_a)^q \rangle \sim C(q) a^{[-\tau(q)-D_0]}$. From Eq. (3), we have $\tau_a(q)+D_0=\tau(q)-\log[C(q)]/\log(a)+D_0$, but the prefactor can be eliminated by computing $\tau_a(q)$ for two different bases. One can then obtain the correct base-dependent exponents for an arbitrary base. Internal consistency requires that all of them should collapse onto a single curve. Figure 3 shows just such a collapse for bases $a=2$, 3, 4, 5, 6, 8, and 10 (where the prefactor was computed using bases 2 and 4). The collapse strongly indicates that there is no preferred base as far as it concerns the scaling properties.

Finally, Fig. 4 compares the scaling exponents for atmospheric flows with those computed [20] from laboratory data. The latter have been computed using conventional box-counting methods and thus do not assume uncorrelated multiplicative processes. The exponents for atmospheric flows have been computed using the multiplier method which uses just such an assumption. The excellent agreement with conventional box counting (in the range where the latter is capable of yielding exponents) indicates the correctness of our convolution arguments based on uncorrelated multiplicative processes. (Such an approach would fail for the period-doubling attractor because the contraction ratios in that case are highly correlated, thus invalidating the simple convolution arguments used here.) We thus observe a nontrivial and interesting empirical fact that the successive multipliers in cascades, which give rise to the observed intermittency in turbulence, seem to be essentially uncorrelated. The comparison in the negative $f(\alpha)$ region shows excellent agreement between the laboratory and atmospheric scaling properties, supporting the conjecture of universal scaling for even the rare events in the small-scale velocity field in fully developed turbulence.

In the past few years a variety of cascade models such as the log-normal model [24], beta model [25], random beta model [26], and p model [8] have been proposed to mimic intermittency in turbulence. None of these models displays sample-to-sample fluctuations or negative dimensions; nor do they explain the multiplier distributions shown in Fig. 2. One can, however, construct an entire family of simple cascade models which display all of the above features and whose $f(\alpha)$ functions agree well with experiment. The simplest model would be a binary model with multipliers picked randomly from a triangular distribution (shown by the solid line in Fig. 2) which is a rough approximation to the mean distribution for a binary cascade. Figure 4 shows that the $f(\alpha)$ function for this model is in good agreement with other experimental data. As already remarked, this cascade model displays the right behavior with respect to sample-to-sample fluctuations shown by circles in Fig. 1. The model also reproduces the observed [20,27] stretched exponential tails, $P(\varepsilon)\sim\exp\{-\beta(\varepsilon)^{1/2}\}$, in the probability distributions of the energy dissipation rate ε. However, it cannot address issues such as the divergence of high-order moments.

We thank J. Eggers, C. J. Evertsz, R. V. Jensen, P. W. Jones, L. P. Kadanoff, B. B. Mandelbrot, C. Meneveau, M. Nelkin, N. Read, and G. Stolovitzky for useful dis-

cussions. A.B.C. acknowledges support from ONR and the Materials Research Laboratory at the University of Chicago. K.R.S. acknowledges support from an AFOSR grant.

[1] E. A. Novikov, Prikl. Mat. Mekh. **35**, 266 (1971) [Appl. Math. Mech. **35**, 231 (1971)]; Phys. Fluids A **2**, 814 (1990). The 1971 paper, which has largely gone unnoticed in the context of multifractals, dealt with cascade models and the importance of multipliers in turbulence. Much of that paper translates easily into the multifractal framework.

[2] B. B. Mandelbrot, J. Fluid Mech. **62**, 331 (1974).

[3] H.G.E. Hentschel and I. Procaccia, Physica (Amsterdam) **8D**, 435 (1983).

[4] U. Frisch and G. Parisi, in *Turbulence and Predictability of Geophysical Fluid Dynamics and Climate Dynamics*, edited by M. Ghil, R. Benzi, and G. Parisi (North-Holland, New York, 1985), p. 84.

[5] T. C. Halsey, M. H. Jensen, L. P. Kadanoff, I. Procaccia, and B. I. Shraiman, Phys. Rev. A **33**, 1141 (1986).

[6] J. P. Eckmann and D. Ruelle, Rev. Mod. Phys. **57**, 617 (1985).

[7] P. Meakin, A. Coniglio, H. E. Stanley, and T. Witten, Phys. Rev. A **34**, 3325 (1986).

[8] C. Meneveau and K. R. Sreenivasan, Phys. Rev. Lett. **59**, 797 (1987); R. R. Prasad, C. Meneveau, and K. R. Sreenivasan, Phys. Rev. Lett. **61**, 74 (1988); K. R. Sreenivasan, Annu. Rev. Fluid Mech. **23**, 539 (1991).

[9] M. J. Feigenbaum, J. Stat. Phys. **25**, 669 (1978).

[10] M. J. Feigenbaum, J. Stat. Phys. **46**, 925 (1987).

[11] A. B. Chhabra, R. V. Jensen, and K. R. Sreenivasan, Phys. Rev. A **40**, 4593 (1989).

[12] A. B. Chhabra and K. R. Sreenivasan, Phys. Rev. A **43**, 1114 (1991).

[13] A. B. Chhabra and K. R. Sreenivasan, in *New Perspectives in Turbulence*, edited by L. Sirovich (Springer, Berlin, 1991).

[14] A. B. Chhabra and R. V. Jensen, Phys. Rev. Lett. **62**, 1327 (1989).

[15] The same striking phenomenon has been observed in the scaling properties of DLA (unpublished joint work with C. J. Evertsz).

[16] One may argue that the fluctuations disappear in the limit of infinite levels of refinement. However, even geophysical turbulent flows have no more than about a dozen steps in the cascade. Solar turbulence has about 30. Thus one is always dealing with statistical mechanics of small systems and the thermodynamic limit is strictly never reached.

[17] B. B. Mandelbrot, J. Stat. Phys. **34**, 895 (1984).

[18] M. E. Cates and T. A. Witten, Phys. Rev. A **35**, 1809 (1987).

[19] B. B. Mandelbrot, in *Fractals: Proceedings of the Erice Meeting*, edited by L. Pietronero (Plenum, New York, 1989).

[20] C. Meneveau and K. R. Sreenivasan, J. Fluid Mech. **224**, 429 (1991).

[21] K. R. Sreenivasan, Proc. R. Soc. London A **434**, 165 (1991).

[22] In general, whenever $P(M)$ falls off slower than exponentially, e.g., as M^{-p}, moments of order less than $-(p+1)$ will diverge. Concave-shaped $P(M)$ will result in divergences for positive p values.

[23] C. W. Van Atta and T. T. Yeh, J. Fluid Mech **59**, 537 (1973); **71**, 417 (1975).

[24] A. N. Kolmogorov, J. Fluid Mech. **13**, 82 (1962).

[25] U. Frisch, P. L. Sulem, and M. Nelkin, J. Fluid Mech. **87**, 719 (1978).

[26] R. Benzi, G. Paladin, G. Parisi, and A. Vulpiani, J. Phys. A **17**, 3521 (1984).

[27] P. Kailasnath, K. R. Sreenivasan, and G. Stolovitzky, Phys. Rev. Lett. (to be published).

[28] For these computations, we simulated 720 different realizations of a binary multiplicative process with ten steps in each cascade. We calculated multiplier distributions assuming cascades of different bases, and eliminated the base-dependent prefactor in the same manner as for the turbulence data. We note that the exponents so calculated are somewhat different from those evaluated analytically from triangular multiplicative process with unity prefactor. For the present, we do not understand the proper method of analytically estimating these prefactors or of reconciling these differences completely satisfactorily.

Probability Density of Velocity Increments in Turbulent Flows

P. Kailasnath, K. R. Sreenivasan, and G. Stolovitzky
Mason Laboratory, Yale University, New Haven, Connecticut 06520-2159
(Received 22 January 1992)

Measurements have been made of the probability density function (PDF) of velocity increments $\Delta u(r)$ for a wide range of separation distances r. Stretched exponentials provide good working approximations to the tails of the PDF. The stretching exponent varies monotonically from 0.5 for r in the dissipation range to 2 for r in the integral scale range. Theoretical forms based on multifractal notions of turbulence agree well with the measured PDFs. When the largest scales in the velocity u are filtered out, the PDF of $\Delta u(r)$ becomes symmetric and, for large r, close to exponential.

PACS numbers: 47.25.−c, 02.50.+s, 03.40.Gc, 05.45.+b

Much work in the turbulence literature [1–4] has been devoted to the determination of the scaling properties of the structure functions $\langle[\Delta u(r)]^n\rangle$, where n is a positive integer and $\Delta u(r)$ is the velocity increment between two spatial locations which are a distance r apart. It has recently [5] been emphasized that a better strategy may be to focus on the probability density functions (PDF's) of $\Delta u(r)$, $p_{\Delta u}(\Delta u)$, rather than on the collection of moments. Accordingly, this Letter is concerned with the PDFs of $\Delta u(r)$ and of velocity derivatives, and has three purposes. First, it provides experimental data on $p_{\Delta u}(\Delta u(r))$ for a large range of separation distances r spanning the dissipation range on one end and the integral scale range on the other. The data show that the PDFs are square-root exponential for r in the dissipation range and Gaussian for r on the order of the correlation (or the integral) scale. Second, it provides for the PDFs a theoretical expression based on the multifractal picture for turbulence dynamics. The third aspect is related to the exact result known for velocity increments [6], namely, that in locally homogeneous turbulence, the third-order structure function in the inertial range obeys the relation

$$\langle[\Delta u(r)]^3\rangle = -\tfrac{4}{5}\langle\varepsilon\rangle r. \qquad (1)$$

While the implications of the nonzero value of $\langle[\Delta u(r)]^3\rangle$ have not been understood fully, it has been shown recently [7] that the removal of the largest scales by high-pass filtering renders the PDF of Δu symmetric. This Letter provides experimental results on the $p_{\Delta u}$ when the low-frequency (or large scale) components of u have been filtered out. For complementary results on PDFs of velocity derivatives and increments, see Refs. [8] and [9]. We shall subsequently return to some of this work.

Measurements were made in the atmospheric surface layer about 6 m above a wheat canopy in the Connecticut Agricultural Research Station. Data were also acquired about 2 m above the roof of a four-story building. The laboratory data were acquired at a height of 0.2δ, where δ is the thickness of the boundary layer, over a smooth flat plate. The boundary-layer-thickness Reynolds number at the measuring station was 32000. Velocity fluctuations were measured using the standard hot-wire (5 μm diam, 0.6 mm length) velocimeter operated in the constant-temperature mode on a DISA 55M01 anemometer. The anemometer voltage was digitized on a 12-bit digitizer and linearized before further processing. Velocity derivatives were obtained by central differencing of the data. Taylor's frozen flow hypothesis was used in interpreting time intervals as space intervals. The precise limitations of this hypothesis are unclear (in spite of much work), especially for the tails of the PDF, but it should be noted that the mean convection velocity in the present experiments was about 15 times larger than the standard deviation of the fluctuating velocity. For obtaining the PDF of the filtered data, a linear phase filter with excellent cutoff characteristics [10] was used.

We have fitted stretched exponentials, $p_{\Delta u} \sim \exp(-\alpha|\Delta u|^m)$, to the tails of $p_{\Delta u}(\Delta u)$. The inset to Fig. 1 demonstrates, for one arbitrarily chosen r, that

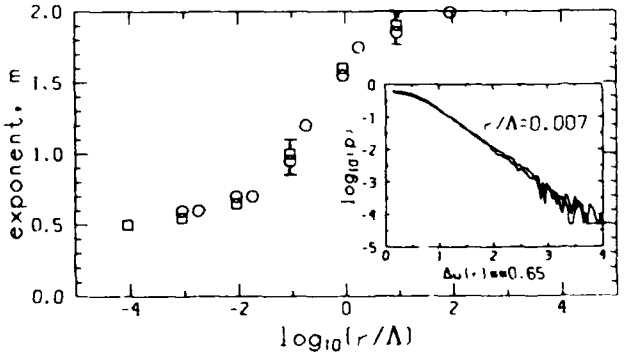

FIG. 1. The experimentally determined stretching exponent m in $p_{\Delta u}(\Delta u(r)) \sim \exp[-\alpha(\Delta u)^m]$, plotted as a function of r/Λ. ○ and □ are for two different sets of atmospheric data. The Taylor microscale Reynolds number R_λ was on the order of 1500 for both. The laboratory data, not plotted here, show a similar trend and roughly coincide with the atmospheric data. $\Delta u(r)$ is obtained by taking the velocity differences separated by a time difference Δt, and interpreting $r = -\Delta t\, U$, where U is the mean velocity of the flow at the measurement station (Taylor's frozen flow hypothesis). The integral scale Λ was determined by obtaining the area under the autocorrelation function of u, and converting it to a length scale by Taylor's hypothesis. Inset: The stretched exponential is a good approximation to typical experimental data for both sides of the distribution. In this figure and others in this paper, Δu is normalized by its root-mean-square value.

there is an extensive region of the PDF to which a stretched-exponential fit is good. It follows from Eq. (1) that there must be a certain asymmetry between the two tails of the distribution, but this asymmetry is not very large. In fact, Fig. 1 shows that the differences between the two tails of the distribution, insofar as they relate to the stretched-exponential fits, are small. We shall therefore momentarily ignore this asymmetry and return to it later. The empirically determined stretching exponents are plotted in Fig. 1 as a function of r for two sets of atmospheric data. While square-root-exponential fits are good for r in the dissipation range, Gaussian fits are appropriate for $r \simeq L_0 \sim 10\Lambda$, where Λ is the autocorrelation length scale of u (see caption to Fig. 1). This latter result is not surprising because velocities at two widely separated points become independent of each other. The exponent m increases monotonically through the inertial range. Laboratory data, not displayed here, show a similar behavior.

It should be noted that a somewhat similar effort for temperature increments in a Rayleigh-Bénard convection experiment has been made in Ref. [11].

In a recent paper [9], Benzi *et al.* derived an expression for the PDF of velocity increments. They assumed that $\Delta u(r)$, for r in the inertial range, is given by the random β model [12],

$$\Delta u(r) = \Delta u_0 (r/L)^{1/3} \prod_{i=1}^{n} \beta_i^{-1/3}, \tag{2}$$

where Δu_0 is the characteristic velocity increment on the macroscopic length L_0, and the β_i's are identically distributed independent random variables. Benzi *et al.* [9] used a special case in which the probability density of β was assumed to be given by

$$p_\beta(\beta) = \alpha\delta(1-\beta) + (1-\alpha)\delta(B-\beta), \tag{3}$$

with $\alpha = \frac{7}{8}$ and $B = \frac{1}{2}$, in conformity with experiments [2,3]. Under the further assumption that Δu_0 is normally distributed (see Fig. 1), Benzi *et al.* [9] showed that the PDF of Δu is given by

$$p_{\Delta u}(\Delta u(r)) = \sum_{k=0}^{n} C_k^n \alpha^{n-k} (1-\alpha)^k B^k \frac{1}{(2\pi\sigma_{k;n}^2)^{1/2}} \exp\left[-\frac{\Delta u^2}{2\sigma_{k;n}^2}\right] + \{1 - [\alpha + (1-\alpha)B]^n\}\delta(\Delta u), \tag{4a}$$

$$\sigma_{k;n} = \frac{\langle \Delta u_0^2 \rangle^{1/2} (r/L)^{1/3}}{B^{k/3}}. \tag{4b}$$

Here, n is the number of steps assumed to occur in a cascade before reaching a scale r and is given, for a binary cascade, by $n = \log_2(L_0/r)$. Notice that the second term on the right-hand side of Eq. (4a) accounts for inactive eddies, i.e., spatial regions where the dissipation of energy is zero. Away from $\Delta u = 0$, the first term on the right-hand side of Eq. (4a) is the only contribution to the total PDF.

An alternative expression can be obtained for $p_{\Delta u}(\Delta u(r))$ as follows. Following Kolmogorov [13] we assume that for r in the inertial range of scales

$$\Delta u(r) = v(r\varepsilon_r)^{1/3}, \tag{5}$$

where v is a "universal" stochastic variable, and $r\varepsilon_r$ is the total energy dissipation in the linear piece of size r. It is clear that within this framework [14] any reasonable model for ε_r and v will also yield a reasonable model for the PDF of $\Delta u(r)$. A convenient model [15] for the energy dissipation is one in which the average energy flux summed over any box of size $r/L_0 = 2^{-n}$ can be written as

$$r\varepsilon_r = L_0\varepsilon_0 \prod_{i=1}^{n} m_i, \tag{6}$$

where the multipliers m_i are identically distributed independent random variables. Here $\varepsilon_0 L_0$ is the typical energy dissipation contained in an eddy at the macroscopic scale (or, equivalently, the total energy flux across scales). Noting that $\langle \Delta u_0^2 \rangle \sim (L_0\varepsilon_0)^{2/3}$, we write

$$\Delta u(r) = v\langle \Delta u_0^2 \rangle^{1/2} \prod_{i=1}^{n} m_i^{1/3}. \tag{7}$$

Recalling again from Fig. 1 that $p_{\Delta u}(\Delta u_0)$ is Gaussian (with mean 0 and variance $\langle \Delta u_0^2 \rangle^{1/2}$), we obtain from Eq. (7), with $n = 0$, that *the universal stochastic variable v has a normal distribution with zero mean and unity variance.* In stating this result, we are stretching the validity of Eq. (5) all the way to the integral scales of motion.

Now, Meneveau and Sreenivasan [16] have shown that the following simple model (the so-called p model) for the probability density of m is adequate for most purposes:

$$p_m(m) = 0.5[\delta(m-M) + \delta(m-(1-M))] \tag{8}$$

with $M = 0.3$. Using the normality of v and Eq. (8), we get from Eq. (7) that

$$p_{\Delta u}(\Delta u(r)) = \sum_{k=0}^{n} C_k^n 2^{-n} \frac{1}{(2\pi\sigma_{k;n}^2)^{1/2}} \exp\left[-\frac{\Delta u^2}{2\sigma_{k;n}^2}\right], \tag{9a}$$

$$\sigma_{k;n} = \langle \Delta u_0^2 \rangle^{1/2} M^{k/3} (1-M)^{(n-k)/3}. \tag{9b}$$

Figure 2 shows comparisons between the experimental data for two values of r ($r/\Lambda = 0.009$ in the inertial range and $r/\Lambda = 0.9$) and the theoretical results of Eqs. (4) and (9). The appropriate values of n to be used in Eqs. (4) and (9) are determined by the relation $n = \log_2(L_0/r)$.

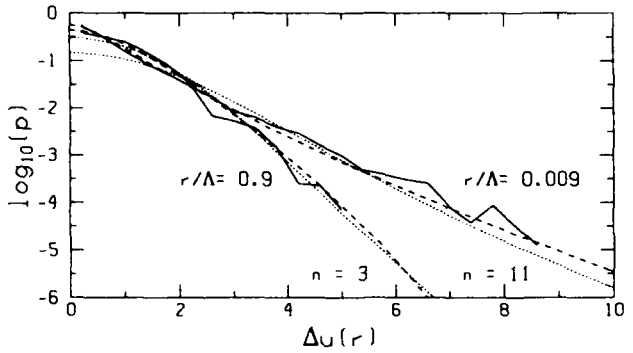

FIG. 2. A comparison between the experimental data for $p_{\Delta u}(\Delta u)$ for two values of r, and Eq. (9) based on the p model (dashed line) and Eq. (4) based on the random β model (dotted line). The formula based on the random β model tends to underestimate the PDF of Δu close to 0.

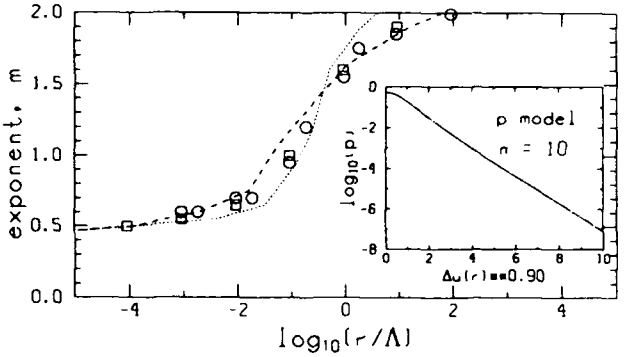

FIG. 4. The stretching exponent m determined empirically for Eqs. (4) and (9), compared with the experimentally determined data of Fig. 1 (dashed line, p model; dotted line, β model). The parameter n is determined arbitrarily by matching the experiment with the theoretical formulas for some r/Λ. Inset: An example in which Eq. (4) for $n=10$ (corresponding to $r/\Lambda=0.009$) is well fitted by a stretched exponential with stretching exponent $m=0.9$.

Both expressions fit the data reasonably well, but the theoretical curve for the random β model falls below the experimental data in the region near $\Delta u=0$. This is so because in this model the active zones ($\Delta u\neq 0$) tend to become more sparse as n increases.

Equation (9) expresses the probability of finding a velocity increment Δu at a fixed scale r. The probability of finding a "gradient" $s=\Delta u/r$ at the scale r can be written, by a change of variables from Δu to s, as

$$P(s|r)=rp_{\Delta u}(rs)\,, \tag{10}$$

where $p_{\Delta u}$ is given by Eq. (9) or Eq. (4). The quotation marks for the gradient above reflect the fact that s is the gradient only when r is comparable to the dissipation scale r_D defined by

$$r_D\Delta u(r_D)/\nu=1\,. \tag{11}$$

Note that the average value $\langle r_D\rangle$ of r_D is the Kolmogorov scale η. For the p model, Eq. (11) becomes

$$r(\langle\Delta u_0^2\rangle^{1/2}L_0/\nu)M^{k/3}(1-M)^{(N-k)/3}2^{-N}=1\,. \tag{12}$$

Here, we have used the relation $r_D/L_0=2^{-N}$, and k, which lies between 0 and N, is randomly picked for the p model from a binomial distribution. Equation (12) and the knowledge of the PDFs of r and k will allow us to compute the probability that the dissipation scale is r_D. Let $P_{r_D}(r)$ be the probability that the dissipation scale is r. The probability density for the gradient can now be written from Eq. (10) as

$$p_s(s)=\int dr\,P(s|r)P_{r_D}(r)\,, \tag{13}$$

where we have weighted the conditional expectation $P(s|r)$ by the probability that the dissipation scale is r. This step, while rigorous, would necessitate cumbersome computations. We avoid them here by making the simplifying assumption that

$$p_s(s)\sim P(s|r=r_D)\,. \tag{14}$$

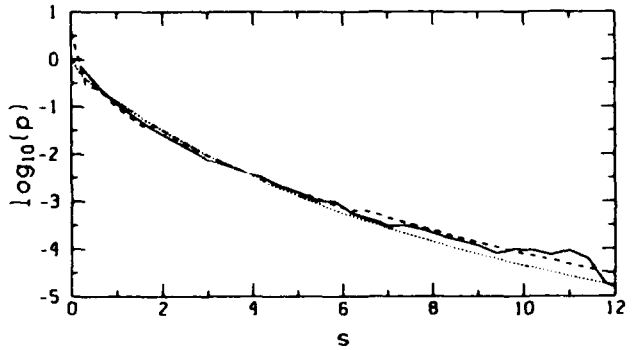

FIG. 3. A comparison between the experiment for the tails of the $p_s(s)$ (solid line) and the theoretical formulas based on the p model (dashed line) and the random β model (dotted line).

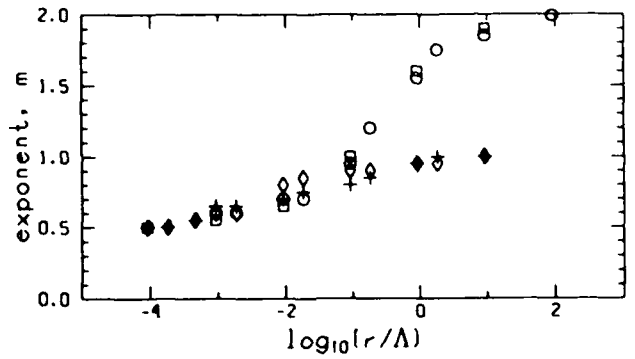

FIG. 5. Demonstration that the PDFs of increments $u_>$, which is the velocity u from which the low-frequency components are removed, tend to an exponential form for large r. This is in contrast to the unfiltered data for which the asymptotic form is nearly Gaussian. The high-pass-filter setting is 30 Hz for + and 9 Hz for ◇. The error bars are comparable to the typical ones shown in Fig. 1.

Noting that $r_D = (\nu/s)^{1/2}$, Eqs. (10) and (14) allow us to express $p_s(s)$ for the p model as

$$p_s(s) \sim \sum_{k=0}^{N(s)} C_k^{N(s)} \frac{1}{M^{k/3}(1-M)^{[N(s)-k]/3}|s|} \exp\left(-\frac{\nu|s|}{2(\Delta u_0^2)M^{2k/3}(1-M)^{2[N(s)-k]/3}}\right) \tag{15}$$

(to within a normalization constant). Note that, in Eq. (15), $N(s) = \frac{1}{2}\log_2(L_0^2|s|/\nu)$ and that the approximate sign in Eqs. (14) and (15) is a reminder about their heuristic nature. Using these same assumptions, Benzi *et al.* [9] derived a similar expression for the PDF of the velocity gradient on the basis of the random β model. Figure 3 shows a comparison between experiment and Eq. (15) and an alternative formula due to Benzi *et al.* [9]. The p model yields a slightly better fit to the data.

We now point out that the stretched exponentials approximate Eqs. (4) and (9) even though the latter two are substantially more complex. This is illustrated in the inset to Fig. 4 where Eq. (9) for $n = 10$ is plotted against $(\Delta u)^{0.9}$. The tails of the PDF are closely approximated by a stretched exponential, consistent with Figs. 1 and 2. The theoretical expressions have been examined for various n, and the stretching exponents m are determined from the best empirical fits [17]. For the stretched exponentials $p_{\Delta u}(\Delta u) = p_{\Delta u}(0)\exp(-a|\Delta u|^m)$, reasonably good straight lines can be fitted to the plot of $\log\{\log[p_{\Delta u}(0)/p_{\Delta u}(\Delta u)]\}$ vs $\log(|\Delta u|)$ in the range of $|\Delta u|$ between the minimum and maximum of $\sigma_{k:n}$ [see Eqs. (4b) and (9b)]. The exponents so determined are plotted in Fig. 4 by matching with experimental data at one chosen location. The fits are good on the whole.

We now return to the asymmetry of the PDF of $\Delta u(r)$. In an earlier work [7], the velocity signal u was decomposed into its Fourier modes, and the modes below the low-frequency end of the inertial range were eliminated. The remaining Fourier modes were recombined to give the filtered signal, say $u_>$. The increments $\Delta u_>(r) = u_>(x+r) - u_>(x)$ were then found to be symmetrically distributed. By fitting stretched exponentials to the tails of the $p_{\Delta u}(\Delta u_>)$, we found that the exponents were similar to those of the unfiltered data in the dissipation range, but tended towards an exponential for large r (Fig. 5). An inquiry on the exponential behavior of the tails of the PDFs of the temperature field has recently been undertaken [18], but it is not clear whether similar explanations hold for velocity increments in the filtered signal.

G.S. thanks Dr. Mille and Dr. Wolf Goodman for their constant encouragement. This research was supported by the Air Force Office of Scientific Research.

[1] See A. S. Monin and A. M. Yaglom, *Statistical Fluid Mechanics* (MIT Press, Cambridge, MA, 1971), Vol. 2, and references cited therein; also F. N. Frenkiel and P. S. Klebanoff, Boundary Layer Met. **8**, 173 (1975).

[2] F. Anselmet, Y. Gagne, E. J. Hopfinger, and R. A. Antonia, J. Fluid Mech. **140**, 63 (1984).

[3] C. Meneveau and K. R. Sreenivasan, J. Fluid Mech. **224**, 423 (1991); K. R. Sreenivasan, Proc. R. Soc. London A **434**, 165 (1991).

[4] P. Tong and W. I. Goldburg, Phys. Fluids **31**, 2841 (1988); P. Constantin, I. Procaccia, and K. R. Sreenivasan, Phys. Rev. Lett. **67**, 1739 (1991).

[5] R. H. Kraichnan, *New Perspectives in Turbulence*, edited by L. Sirovich (Springer-Verlag, Berlin, 1991), pp. 1–54; H. Chen, S. Chen, and R. H. Kraichnan, Phys. Rev. Lett. **63**, 2657 (1989); Y. G. Sinai and V. Yakhot, Phys. Rev. Lett. **63**, 1962 (1989).

[6] A. N. Kolmogorov, Dokl. Akad. Nauk SSSR **32**, 19 (1941).

[7] P. Kailasnath, A. A. Migdal, K. R. Sreenivasan, V. Yakhot, and L. Zubair (to be published).

[8] B. Castaing, Y. Gagne, and E. J. Hopfinger, Physica (Amsterdam) **46D**, 177 (1990).

[9] R. Benzi, L. Biferale, G. Paladin, A. Vulpiani, and M. Vergassola, Phys. Rev. Lett. **67**, 2299 (1991).

[10] A. V. Openheim and R. W. Schafer, *Digital Signal Processing* (Prentice Hall, Englewood Cliffs, NJ, 1975).

[11] E. S. C. Ching, Phys. Rev. A **44**, 3622 (1991).

[12] R. Benzi, G. Paladin, G. Parisi, and A. Vulpiani, J. Phys. A **17**, 3521 (1984).

[13] A. N. Kolmogorov, J. Fluid Mech. **13**, 82 (1962).

[14] In a recent paper [I. Hosokawa and K. Yamamoto, Phys. Fluids A **4**, 457 (1992)], the validity of Kolmogorov's refined similarity hypothesis, Eq. (5), has been criticized. This work raises more questions than it answers, and will be examined elsewhere.

[15] A. B. Chhabra and K. R. Sreenivasan, Phys. Rev. A **43**, 1114 (1991); (to be published).

[16] C. Meneveau and K. R. Sreenivasan, Phys. Rev. Lett. **59**, 1424 (1987).

[17] It might seem strange that Eqs. (4) and (9), being sums of Gaussian distributions, yield a stretched-exponential behavior. However, it is possible to show rigorously that under conditions that are not too restrictive, any arbitrary PDF can be obtained as a suitably weighted integral over normalized Gaussian functions.

[18] Jayesh and Z. Warhaft, Phys. Rev. Lett. **67**, 3503 (1991); J. P. Gollub, J. Clarke, M. Gharib, B. Lane, and O. N. Mesquita, Phys. Rev. Lett. **67**, 3507 (1991).